Eur. J. Biochem. **270**, 3904–3915 (2003) © FEBS 2003 doi:10.1046/j.1432-1033.2003.03772.x

The isolation and characterization of cytochrome *c* nitrite reductase subunits (NrfA and NrfH) from *Desulfovibrio desulfuricans* ATCC 27774

Re-evaluation of the spectroscopic data and redox properties

Maria Gabriela Almeida[1], Sofia Macieira[2], Luisa L. Gonçalves[1], Robert Huber[2], Carlos A. Cunha[1], Maria João Romão[1], Cristina Costa[1], Jorge Lampreia[1], José J. G. Moura[1] and Isabel Moura[1]

[1]*REQUIMTE, CQFB, Departamento de Química, Faculdade de Ciências e Tecnologia, Universidade Nova de Lisboa, Portugal;* [2]*Max-Planck-Institut für Biochemie, Abt. Strukturforschung, Martinsried, Germany*

The cytochrome *c* nitrite reductase is isolated from the membranes of the sulfate-reducing bacterium *Desulfovibrio desulfuricans* ATCC 27774 as a heterooligomeric complex composed by two subunits (61 kDa and 19 kDa) containing *c*-type hemes, encoded by the genes *nrfA* and *nrfH*, respectively. The extracted complex has in average a 2NrfA:1NrfH composition. The separation of ccNiR subunits from one another is accomplished by gel filtration chromatography in the presence of SDS. The amino-acid sequence and biochemical subunits characterization show that NrfA contains five hemes and NrfH four hemes. These considerations enabled the revision of a vast amount of existing spectroscopic data on the NrfHA complex that was not originally well interpreted due to the lack of knowledge on the heme content and the oligomeric enzyme status. Based on EPR and Mössbauer parameters and their correlation to structural information recently obtained from X-ray crystallography on the NrfA structure [Cunha, C.A., Macieira, S., Dias, J.M., Almeida, M.G., Gonçalves, L.M.L., Costa, C., Lampreia, J., Huber, R., Moura, J.J.G., Moura, I. & Romão, M. (2003) *J. Biol. Chem.* 278, 17455–17465], we propose the full assignment of midpoint reduction potentials values to the individual hemes. NrfA contains the high-spin catalytic site (−80 mV) as well as a quite unusual high reduction potential (+150 mV)/low-spin *bis*-His coordinated heme, considered to be the site where electrons enter. In addition, the reassessment of the spectroscopic data allowed the first partial spectroscopic characterization of the NrfH subunit. The four NrfH hemes are all in a low-spin state ($S = 1/2$). One of them has a g_{max} at 3.55, characteristic of *bis*-histidinyl iron ligands in a noncoplanar arrangement, and has a positive reduction potential.

Keywords: nitrite reductase subunits; *c*-type hemes; EPR; Mössbauer; redox potentials.

The multiheme nitrite reductase (ccNiR) catalyses the direct conversion of nitrite to ammonia in a six-electron transfer reaction. It is a key enzyme involved in the second and terminal step of the dissimilatory nitrate reduction pathway of the nitrogen cycle and plays an important role on bacterial respiratory energy conservation [1,2]. It was first isolated in 1981 from the sulfate-reducing bacterium *Desulfovibrio desulfuricans* ATCC 27774 [3], when grown anaerobically in nitrate, instead of sulfate. Since then, a number of respiratory ammonia-forming ccNiRs have been isolated from several nitrate-grown bacteria as *Escherichia coli* K-12 [4], *Vibrio alginolyticus* [5], *Vibrio fisheri* [6], *Wolinella succinogenes* [7] and *Sulfurospirillum deleyianum* [8]. Although not completely characterized, the iron-reducing bacterium *Geobacter metallireducens* also exhibits cytochrome *c* nitrite reductase activity [9]. Recently, another ccNiR was purified from the sulfate reducer *Desulfovibrio vulgaris* Hildenborough, a microorganism not capable of growing in nitrate [10], suggesting that the reported nitrite reducing activity of *Desulfovibrio gigas* sulfate-grown cells [11] can also be attributed to a ccNiR. For a long time, all ccNiRs were wrongly described as approximately 60 kDa monomeric proteins containing six *c*-type heme prosthetic groups, as judged by pyridine hemochrome assays and iron content determinations using the mature protein. However, in 1993, the DNA sequence of the structural gene (*nrfA*) for *E. coli* K-12 ccNiR was published by Darwin *et al.* showing four conventional *c*-type heme binding motifs (CXXCH) which led the authors to consider it as a tetraheme cytochrome [12]. Immediately after, new biochemical analyses on ccNiRs from *W. succinogenes* and *S. deleyianum* also support this result [13]. Later on, the reinvestigation of the sequence data of the *E. coli* K-12 enzyme revealed another heme group attached to the protein by a novel motif, where the histidine residue was replaced by a lysine (CXXCK). It was than established that *E. coli* K-12 ccNiR contains five

Correspondence to I. Moura, Depart. de Química, Faculdade de Ciências e Tecnologia, Universidade Nova de Lisboa, Quinta da Torre, 2829–516 Monte de Caparica, Portugal.
Fax: + 351 21 2948550; Tel.: + 351 21 2948381;
E-mail: isa@dq.fct.unl.pt

Abbreviations: ccNiR, cytochrome *c* nitrite reductase; cmc, critical micellar concentration; ICP, inductively coupled plasma.

Note: a web page is available at http://www.dq.fct.unl.pt/bioprot

(Received 21 May 2003, revised 17 July 2003, accepted 28 July 2003)

rather than four covalently bound *c*-type hemes [12]. The resolution of the 3D structural of NrfA isolated from *S. deleyianum* [14] and *W. succinogenes* [15] closed this controversy, definitively establishing the presence of five hemes per molecule. The two structures are nearly identical. Both enzymes crystallize as homodimers where 10 hemes are found in remarkable close packing. Except for the substrate-binding heme CWXCK, which constitutes a new reaction center, the heme core is fairly conserved when compared to other multiheme cytochromes structures, despite low sequence identity and function. The 3D structures of the penta-heme NrfA from *E. coli* K-12 [16] and *D. desulfuricans* ATCC 27774 are also available [17]. In both cases, when compared with *W. succinogenes* and *S. deleyianum* structures, the overall protein architecture is essentially kept.

ccNiR was isolated either as a soluble periplasmic monomer (*V. fisheri*, *E. coli* K-12, *W. succinogenes*, *S. deleyianum*) and/or in an inner membrane associated form (*D. desulfuricans* ATCC 27774, *E. coli* K-12, *W. succinogenes*, *S. deleyianum*, *D. vulgaris* Hildenborough). The work of Shumacher *et al.* in 1994 [13] demonstrated that ccNiR membrane preparations from *S. deleyianum and W. succinogenes* comprise an additional small 22 kDa *c*-type cytochrome subunit, also later identified in *D. desulfuricans* ATCC 27774 [18–20] and *D. vulgaris* Hildenborough [10]. The corresponding gene (*nrfH*) sequence from *W. succinogenes* encodes four heme-binding sites (CXXCH) and a putative helical membrane anchor; presumably, is the physiological redox partner of NrfA [21]. However, in *E. coli* K-12 this role is most likely undertaken by a periplasmic pentahemic cytochrome *c*, NrfB [22].

These important developments demand the re-examination of the biochemical properties of *D. desulfuricans* ATCC 27774 ccNiR, and its implications on the existing spectroscopic data, which are still quite unique among the entire knowledge in the ccNiRs field, but interpreted on the basis of a hexahemic monomeric protein [23,24]. The EPR spectrum (pH 7.6) showed a low-spin ferric heme signal at $g_{max} = 2.96$ and several broad resonances indicative of heme–heme magnetic interactions (absorption-type signal at $g \approx 3.9$ and derivative type-signal with zero-crossing at $g \approx 4.8$). The EPR/redox titrations studies allowed the further detection of a high-spin ferric heme (substrate-binding site), pairwise-coupled ($g \approx 3.9$) to another low-spin heme with $g_{max} = 3.2$ [23]. As shown by Mössbauer measurements, the application of a strong-field (8 T) on ccNiR decoupled all the interacting hemes. Consequently, the corresponding spectra were interpreted as the superposition of six spectral components of equal intensity, originating from six magnetically isolated heme groups. Distinct hyperfine parameters were derived for each individual heme: one is in the high-spin electronic configuration ($S = 5/2$) whilst the remainders five are low-spin ($S = 1/2$) with g_{max} values at 3.6, 3.5, 3.2, 3.0 and 2.96 [23,24].

In this communication, we report for the first time the isolation and biochemical characterization of *D. desulfuricans* ATCC 27774 ccNiR subunits. The stoichiometry between NrfH and NrfA is discussed. The reassessment of previous spectroscopic studies was undertaken, particularly regarding the assignment of spectroscopic and redox potentials of the NrfA hemes. In addition, the first partial spectroscopic and redox characterization of the NrfH subunit is also presented. Up to now, there has been no information of this kind on any NrfH protein.

Materials and methods

Protein purification

ccNiR was purified from *D. desulfuricans* ATCC 27774 membrane fraction as previously described, with slight modifications [25,26]. The soluble fraction was applied onto a DEAE-52 column (XK26, Pharmacia), washed with 10 mM Tris/HCl pH 7.6 and then eluted with a linear gradient of 10–500 mM Tris/HCl. The eluate fraction containing nitrite reductase activity was ultracentrifugated at 40 000 ***g***, for 1 h. The nitrite reductase purity was checked by SDS/PAGE and by UV-Vis spectroscopy.

Biochemical methods

SDS/PAGE was carried out according to Laemmli [27]. The standard proteins used for molecular mass determination were from Bio-Rad (broad-range kit). The gels were stained with Coomassie Brillant Blue or with silver nitrate [28] if required. We also performed heme peroxidase [29] and nitrite reductase activity staining [30]; in both cases the sample buffer did not contain the reductive agent dithiotreitol and, for nitrite reductase activity, the protein samples were not boiled. Protein content was determined with the Bicinchoninic Acid Protein Assay Kit (Pierce), using horse heart cytochrome *c* as standard (Sigma). The relative molecular mass of the ccNiR complex as purified was estimated on a prepacked Superose 6 column 10/30 H (Pharmacia; separation range, 5–5000 kDa) with a mobile phase of 100 mM NaCl in 50 mM Tris/HCl (pH 7.6). Standard proteins from Pharmacia and Sigma were used for column calibration. The number of heme groups per monomer was determined as alkaline pyridine hemochromes using an extinction coefficient of ε_{550nm} (red) = 29.1 mM·cm^{-1} [31], and by iron content as given by plasma emission spectroscopy, using an inductively coupled plasma (ICP) source (Jobin Yvin-Horiba); the standards were from Reagecom.

Subunit separation

In order to separate the individual ccNiR components, protein samples were directly applied onto a Superdex 200 10/30 H (Pharmacia; separation range, 10–600 kDa) gel filtration column, equilibrated and eluted in 0.1 M Tris/HCl, pH 7.6 and several common protein–protein dissociation salts (1 M sodium chloride, 8 M urea and 6 M guanidinium chloride) and ionic detergents (CHAPS, Zwittergent 3–10, Zwittergent 3–16 and SDS); the concentrations were to 2 or 4 times the critical micellar concentration (cmc). The chromatograms were registered following the absorbance simultaneously at 220 nm and 409 nm. All reagents were from Merck, except Chaps, Zwittergent 3–10 and Zwittergent 3–16 that were purchased from Calbiochem. The excess SDS was removed from samples using the Calbiosorb^{TM} adsorbent (Calbiochem).

Activity assays

Nitrite reductase activity was determined measuring the enzymatic consumption of nitrite per time unit. The reaction was performed in 0.1 M phosphate buffer, pH 7.6, in the presence of dithionite reduced methyl viologen, at 37 °C [3]. The amount of nitrite left in the reaction mixture was determined by a colorimetric assay, based on the Griess method [32].

Primary Structure

Chemical sequencing. The N-terminal amino-acid sequence of ccNiR subunits and their internal peptides were determined by automated Edman degradation on a Procise™ Protein Sequencer (model 491, Applied Biosystem), composed by a 140C Microgradient Delivery System, a 785-A UV-detector and a 610-A data analysis, following the manufacturer's instructions. Each subunit (0.2–0.3 $mg{\cdot}mL^{-1}$) was enzymatically digested for 18 h at 37 °C with endoproteinase Lys-C (Roche Molecular Biochemicals) in 1 mM EDTA, 25 mM Tris/HCl buffer, pH 8.5, at an enzyme/substrate ratio (E : S) of 1 : 50 (by mass). Similar amounts of native protein were incubated with α-chymotrypsin (Boehringer Mannheim) for 18 h at 25 °C in 100 mM Tris/HCl, pH 8.6, at an E : S = 1 : 50. Peptides were isolated by reverse-phase HPLC on a Lichrospher RP-100 (Merck) column (25 × 0.4 cm, C18, 5 μm particle size).

DNA sequencing. Based on NrfH N-terminal sequence previously acquired by chemical sequencing, the oligonucleotide ccNiR_GTPRNGPW, 5′-GGIACICCIMGIAAYG GICCITGG-3′, was synthesized and used together with the primer ccNiR_Cterm, 5′-TCYTGICCYTCCCASACYT GYTC-3′, already used in *nrfA* isolation [17] to amplify by PCR a 2000 bp DNA fragment comprising *nrfH* and *nrfA* partial genes. The reaction was accomplished in a total volume of 25 μL using 296 μg of genomic DNA as template, 1.5 mM $MgCl_2$, 0.2 mM dNTPs and 2.5 U of *Taq* DNA polymerase (MBI Fermentas). Thermocycler (Stratagene) parameters set were 94 °C for 3 min, 48 °C for 40 s, 72 °C for 10 min, for 36 cycles. The DNA fragment was sequenced by primer walking, using an automated DNA sequencer (Model 373, Applied Biosystems) and the PRISM ready reaction dye deoxy terminator cycle sequencing kit (Applied Biosystems).

The molecular masses of the translated polypeptide chains were calculated with the PROTPARAM tool (http://www.expasy.org/tools/protparam.html). Prediction of transmembrane helices was performed with the program TMHMM 2.0 (http://www.cbs.dtu.dk/services/TMHMM-2.0.html) [33]. The program LIPOP (http://psort.nibb.ac.jp) was used for examination of lipoprotein consensus sequences. NrfH sequence was scanned for cytochrome *c* classes motifs with the program PRINTS33_0 (http://bioinf.man.ac.uk).

Spectroscopy

The electronic and EPR spectra of the separated subunits were recorded in the presence of 1% (w/v) SDS. UV-Visible (UV-Vis) spectra were obtained on a Shimadzu UV-2101 PC spectrophotometer. X-Band EPR measurements were performed on a Bruker EMX EPR spectrometer using a rectangular cavity (Model ER 4102ST) and 100 KHz field modulation field, and equipped with an Oxford Instrument continuous liquid helium flow cryostat.

Results and discussion

Electrophoretic profile

Figure 1A shows the SDS/PAGE of purified ccNiR upon different treatments. The complex dissociates into an intense band of 61 kDa (NrfA) and a band of weak intensity of 19 kDa (NrfH), confirming its hetero-oligomeric nature (Fig. 1, lane 1).

However, in the absence of boiling (Fig. 1A, lanes 2 and 4) high molecular mass bands of approximately 110 kDa and > 200 kDa were visible, as well as a faint band at 37 kDa, suggesting the presence of dimers. All of the bands stained positively for heme *c* (Fig. 1B) but only the high molecular mass bands (≥ 55 kDa) stained for nitrite reducing activity (Fig. 1C). Gel slices containing the ≈ 110 kDa band, boiled in the presence of dithiothreitol and submitted to a new SDS/PAGE, yield single bands at approximately 55–60 kDa (not shown). Moreover, the SDS/PAGE

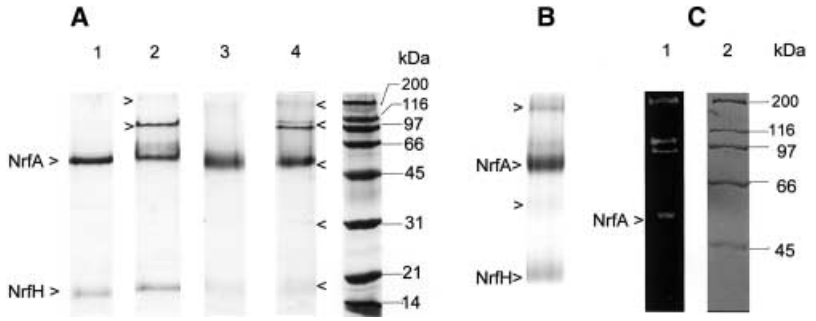

Fig. 1. SDS/PAGE (11% acrylamide) analysis of purified *D. desulfuricans* ATCC 27774 ccNiR membrane complex. (A) Mini-gel of 9 × 9.5 cm. Protein treatment: Lane 1, 0.3 M dithiothreitol, boiling for 1 min; lane 2, 0.3 M dithiothreitol, no boiling; lane 3, no dithiothreitol, boiling for 1 min; lane 4, no dithiothreitol, no boiling; lane 5, standards. The gel was stained with Coomassie Brilliant Blue. (B) Mini-gel of 9 × 9.5 cm. Protein treatment: no dithiothreitol, boiling for 1 min. The gel was stained for heme *c*. (C) Gel of 16 × 18 cm. Protein treatment: no dithiothreitol, no boiling. The gel was stained for nitrite reductase activity.

analyses of NrfA crystals also have shown the high molecular mass bands (not shown). Such electrophoretic behavior suggests that the bands at approximately 110 and 37 kDa correspond to strongly attached dimers of both NrfA (α_2) and NrfH (β_2), respectively. The presence of dithiothreitol (Fig. 1A, lanes 1 and 2) did not affect significantly the electrophoretic profile indicating that disulfide bridges are not involved.

Purification attempt of a soluble form of ccNiR

Nitrite reductase activity was checked in the soluble cell fraction in order to investigate the existence of a soluble monomeric form of ccNiR, as reported on other microorganisms [4,6,13]. Liu and Peck detected almost 50% of the crude extract nitrite reducing activity in the *D. desulfuricans* ATCC 27774 soluble fraction and suggested that most of the activity could be caused by interference of the soluble sulfite reductase [3,25]. Our results have shown a comparable level of nitrite reductase activity in the soluble fraction. In a purification attempt of a soluble ccNiR, this fraction was submitted to ion-exchange chromatography (see Materials and methods) but most of the activity was eluted during the column washing procedure. The collected fraction was slightly viscous and after ultracentrifugation, a membranous pellet was present and the supernatant enzymatic activity dramatically decreased. Thus, nitrite reductase activity in the soluble fraction should be mainly due to resuspended membrane material, not completely sedimented from the viscous cell lysate. We may then conclude that *D. desulfuricans* ATCC 27774 ccNiR is strongly bound to the membrane. However, the sequence of *nrfA* demonstrated that the gene encodes for a precursor of NrfA, which includes an export signal to the periplasma, and no membrane spanning elements were detected when analyzing the primary structure features [17]. On the other hand, analysis of NrfA sequence using the program LIPOP (see Materials and methods) predicted a covalent lipid attachment motif (CQDV) at the mature N-terminus (Fig. 2; full alignment given in [17]); the lipid moiety serves as a hydrophobic anchor for attachment to the membrane.

However, the CQDV segment is not present in NrfA from *W. succinogenes* and *S. deleyianum* (Fig. 2). Simon *et al.* demonstrated that ccNiR complex from *W. succinogenes* is exclusively attached to the membrane by the NrfH subunit [34].

The native molecular mass

The gel filtration chromatogram revealed two unresolved peaks of high molecular mass (890 kDa and higher, data not shown). However, the subunit composition of both fractions seemed to be the same, as judged by their SDS/PAGE profile (essentially, the same as Fig. 1A, lane 1). These results indicate that ccNiR, as purified, is a mixture of high molecular mass multimers.

The ccNiR complex (NrfHA) separation into its components

To explore their molecular mass differences, several attempts to isolate the ccNiR subunits were performed by gel filtration chromatography in the presence of a number of salts and detergents to efficiently break the protein–protein interactions. Sodium chloride (Fig. 3A) was not able to separate the complex. Urea and guanidinium chloride produced an identical elution profile (not shown).

The second screening for complex separation relied on micellar chromatography experiments. In a first attempt, nondenaturating zwitterionic Chaps, a derivative of cholic acid (the detergent used to extract ccNiR from *D. desulfuricans* ATCC 27774 membranes, but less effective at disrupting protein–protein interactions) was used. However, it did not dissociate the monomers efficiently (Fig. 3A). Zwittergent 3–10 (the detergent used for crystallization) was then used. The small subunit is not present in the crystalline material suggesting that dissociation occurred during crystallization [26]. In fact, in the presence of Zwittergent 3–10 the chromatogram displayed important alterations (Fig. 3B), yielding two main peaks of approximately 850 and 162 kDa. The SDS/PAGE examination of the eluted fractions (Fig. 3B, inset) revealed that the large NrfA subunit is present in all fractions, but the small NrfH subunit is difficult to visualize on the polyacrylamide gel as it has an abnormal behavior, probably due to an insufficient Zwittergent 3–10 substitution by SDS. Even so, it seems to be present in both 850 and 162 kDa forms. In this regard, the best combination of the two subunits that match the smallest molecular mass is $\alpha_2\beta_2$. Overnight incubation of the protein in this detergent led to a decrease of the area of the first peak and an increase in the second one. This supports the idea that the high molecular mass ccNiR aggregate slowly dissociates upon Zwittergent 3–10 treatment. As ccNiR crystals took one month to grow, there was enough time to the total separation between the two subunits. Another attempt was made with a similar zwitterionic surfactant, but with a longer hydrophobic alkyl tail, such as Zwittergent 3–16. However, it did not improve the complex separation (Fig. 3A). Finally, we applied a strong denaturant agent, SDS. As shown in Fig. 3C, the ccNiR complex separation into its monomers was completely achieved using this

Fig. 2. *D. desulfuricans* ATCC 27774 NrfA N-terminal sequence alignment. Conserved residues are shaded. ▼, probable signal peptide cleavage site. Numbering refers to the NrfA_Ddes sequence. NrfA_Ddes, NrfA from *D. desulfuricans* ATCC 27774 (EMBL AJ316232); NrfA_Ecoli, NrfA from *E. coli* K-12 (SWISS-PROT P32050); NrfA_Sdel, NrfA from *S. deleyianum* (SWISS-PROT Q9Z4P4); NrfA_Wsuc, NrfA from *W. succinogenes* (TREMBL Q9S1E5). This figure was prepared using PILEUP, in the Wisconsin Package Version 10.0 (Genetics Computer Group, Madison, WI, USA) and ALSCRIPT [55].

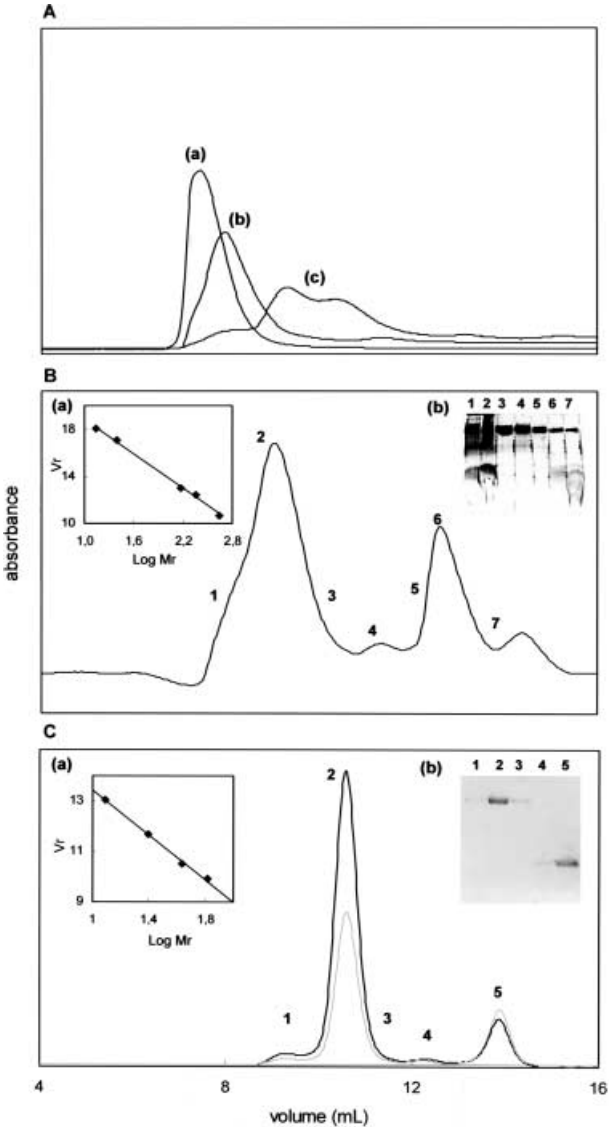

Fig. 3. Gel filtration chromatography of *D. desulfuricans* ATCC 27774 ccNiR on a Superdex 200 10/30 HR column. The column was equilibrated and eluted with 0.1 M Tris/HCl, pH 7.6, in the presence of (A) (a) 1 M NaCl; (b) 1% (v/v) Chaps (2× cmc); (c) 0.0025% (v/v) Zwittergent 3–16 (2× cmc). (B) 5% (v/v) Zwittergent 3–10 (4× cmc). Insets: (a) column calibration with ferritin, catalase, alcohol dehydrogenase, ovalbumin, chymotrypsin and ribonuclease; (b) SDS/PAGE (12.5% acrylamide) of the collected fractions, stained with silver nitrate. (C) 1% SDS (4× cmc). The peak area ratios NrfA/NrfH at 409 nm and 220 nm are roughly 2.8 and 6.9, respectively. Insets: (a) column calibration with cytochrome *c*, chymotrypsin, ovalbumin and bovine serum albumin; (b) SDS/PAGE (12.5% acrylamide) of the collected fractions, stained with silver nitrate. The chromatograms were registered at: A, 409 nm; B, 409 nm; C, 409 nm (black line) and 220 nm (gray line). Flow was 0.3 mL·min^{-1}.

detergent in the elution buffer. According to the column calibration, the molecular masses of the two observed peaks (Table 1) are in good agreement to the NrfA and NrfH molecular masses, as further proved by the respective SDS/PAGE profile (Fig. 3C, inset).

After excess SDS removal from NrfA and NrfH samples with detergent adsorbents, the individual monomers (especially NrfH) exhibited a high tendency to precipitate. Their absorption spectra in the UV region (not shown) led us to suspect that partial degradation occurred. Therefore, these subunits require the presence of a detergent for stabilization. This behavior is typical of integral membrane proteins due to the clustering of their hydrophobic regions.

Heme content

The heme content as given by ICP measurements as well as the hemochromopyridine assays (Table 1) indicate 5 and 4 hemes per NrfA and NrfH molecule, respectively, which is in agreement with the number of hemes predicted from both amino-acid sequences (see below).

Subunit stoichiometry

Densitometry analysis of the 61 kDa and 19 kDa bands (SDS/PAGE stained with Coomassie Brilliant Blue) gave an intensity ratio of two to one, respectively (not shown). The areas comparison of the two SDS-gel filtration chromatographic peaks, measured at 409 nm and 220 nm, gave a proportion of 2.8 and 6.9, respectively (Fig. 3C). Correcting these ratios for the number of hemes (409 nm) and peptide bonds (220 nm) per subunit, it also indicates a stoichiometry of 2NrfA:1NrfH. The gel-filtration experiments were highly reproducible and independent of the protein batch. This set of data suggests a ratio of two NrfA subunits to one NrfH subunit. This prompts us to raise the following questions. As the above experiments were performed in strong denaturant conditions, does the 2 : 1 ratio correspond to the physiological complex stoichiometry? Or does it mean that the extraction procedure results in an incomplete removal of the integral membrane subunit NrfH? The gel filtration micellar chromatography in the presence of Zwittergent 3–10 (Fig. 3B) showed, among other oligomeric species, one important peak at $\approx$ 162 kDa, presumably corresponding to a $\alpha_2\beta_2$ heterodimer i.e. a stoichiometry of 1 : 1. No species revealing a 2 : 1 proportion (multiples of 140 kDa) were recognized. Furthermore, the SDS/PAGE profile suggested the existence of both α_2 and β_2 dimers. Unfortunately, attempts to characterize the oligomeric status of the native complex by MALDI molecular mass measurements in nondenaturing conditions were unsuccessful as both proteins did not ionized (B. Devreese, Universiteit Gent, personal communication); in denaturating conditions, only the two individual subunits were readily apparent (Table 1). These results may be explained if one considers that *D. desulfuricans* ATCC 27774 ccNiR extraction procedure yields an excess of the peripheral NrfA subunit. Thus, we propose that ccNiR is purified as high molecular mass aggregates ($\geq$ 850 kDa), containing the double of NrfA subunit in respect to the NrfH subunit. Nevertheless, inside these huge aggregates there are species of the type $\alpha_2\beta_2$. The present findings are in agreement with the reported isolation of two different forms of ccNiR from *S. deleyianum* membranes: a heterooligomeric high molecular mass complex, containing the two subunits in a proportion of four NrfA to one NrfH, and a low molecular mass form (20–30%) constituted only by the NrfA subunit [13,21].

Table 1. Molecular properties of *D. desulfuricans* ATCC 27774 ccNiR subunits.

	Molecular mass (kDa)					
Subunit	Gel filtration	SDS/PAGE	MALDI	Heme content	Iron content	CXXCH/K motifs
NrfA	67	61	61.34	5.0 ± 1.0	4.5 ± 0.2	5
NrfH	18	19	19.23	3.7 ± 0.2	3.2 ± 0.2	4

Primary structure analysis

The N-terminal sequences of *D. desulfuricans* ATCC 27774 ccNiR subunits obtained by Edman degradation are as follows.

NrfA, 24 XQDVSTELKAPKYKTGIAETETKMSAF KGQF PQQYASYMKNNE.

NrfH, 1 GTPRNGPWLKWLLGGVAAGVVLMGVL AYAM TTTDQRP.

The internal peptide sequences obtained by enzymatic cleavage, as well as the *nrfA* and *nrfH* sequences determined during the course of the chemical sequencing have been submitted to the EMBL database under accession number AJ316232.

The sequence of *nrfA* encodes for a precursor signal peptide [17], which shows the LXXC consensus motif recognized by signal peptidase II (Fig. 2). The peptidase cuts upstream of a cysteine residue to which a glyceride-fatty acid lipid is attached [35], i.e. between Gly23 and Cys24. This cleavage site was experimentally confirmed by the N-terminal sequencing of the mature protein that starts at 24th residue. The program LIPOP also predicted a lipid attachment to Cys24. The deduced amino-acid sequence of NrfA contains four classical *c*-type heme-binding motifs CXXCH and a fifth heme-binding site CWXCK [17]. The predicted molecular mass, excluding the cleaved 23 N-terminal amino acids and the heme prosthetic groups, is 56768 Da. The addition of five hemes gives 59848 Da, slightly lower than the value obtained by MALDI. This could be due to the putative post-translational lipid modification.

The deduced amino-acid sequence of NrfH appears to carry four CXXCH consensus sequences (Fig. 4). It has a predicted molecular mass of 16764 Da, excluding the heme groups. The attachment of four hemes leads to a total molecular mass of 19228 Da, which matches the value given by MALDI (Table 1). Apparently, NrfH is devoided of a periplasm export signal but is predicted to be a transmembrane protein, with the bulk of the protein facing the periplasm. The N-terminus (residues 1–10) remains in the cytosol, while residues 11–33 are predicted to form a transmembrane helix, which most likely acts as a membrane anchor. The tight membrane association and the aggregation propensity after solubilization are probably due to this hydrophobic region. These results were obtained with TMHMM 2.0 (see Materials and methods); the secondary structure prediction servers DAS and JPRED, available at http://www.expasy.org, revealed similar profiles.

Alignment and homology

The data on alignment and homology of NrfA was discussed in reference [17]. NrfH is homologous to the proteins of the NapC/NirT family, which has an overall similarity of approximately 30% (Fig. 4). Cytochromes belonging to this family act as electron mediators between the quinol pool and a sort of periplasmic terminal acceptors as nitrate reductase, dimethylsulfoxide reductase, trimethylamine *N*-oxide reductase, cytochrome cd_1 nitrite reductase and fumarate reductase [1]. The infrared-MCD and EPR analysis of the water-soluble heme domain of an expressed NapC from *Paracoccus denitrificans* [36] indicated that the four heme irons have *bis*-histidinyl coordination.

Except for the first heme-binding site, CASCH, three of NrfH heme binding sites have class III cytochrome *c* signature (results obtained with PRINTS33_, see Materials and methods). This class is typically dominated by the cytochrome c_3 superfamily from *Desulfovibrio* genus [37,38]. A number of tetrahemic cytochromes c_3 (13 kDa) [39,40], dimeric c_3 (26 kDa) [41] and the trihemic c_7 [42,43] have their three-dimensional structure already solved, which prompted us to investigate if the spatial orientation of at least three of the four NrfH hemes could follow the heme arrangements observed in cytochrome c_3 superfamily, and if the crystal structures of either cytochrome c_3 or cytochrome c_7 could be used for modelling. However, no significant similarity between NrfH and c_3 primary structures was observed outside the heme attachment sites (Fig. 4).

As shown in Fig. 4, the sequence pattern LGG-X_3-GV-X_3-G-X_4-A-X_3-T-X_2-E(R)-X-FCXSCHXM present in *D. desulfuricans* ATCC 27774 NrfH is highly conserved in the membrane-anchored NapC available in databases. This segment comprises the putative transmembrane α-helix and the heme-binding site that does not share cytochrome class III signature. Strikingly, some residues (Ala, Thr, Glu, Phe, Ser, His and Met) were implicated in the quinone coordination at transmembrane domains of several electron-chain complexes. No crystallographic data or mutagenic analyses are currently available for quinone binding cytochromes *c*, making difficult a feasible identification of new Q sites. Although quinone binding sites show a wide variability, several aspects seem to be conserved [44,45]. Aromatic and aliphatic residues sometimes flank the quinone ring and it is generally observed that quinone/quinol binds into hydrophobic sites essentially by hydrogen bonding between the carbonil/hydroxil head groups and a positive charged amino acid [44,46]. Indeed, His is frequently identified as a critical amino acid for proper quinone interaction [44]. For example, formate dehydrogenase-N from *E. coli* K-12, whose 3D structure was recently determined, has a membrane-spanning diheme containing subunit that binds a quinone molecule through the His ligand of heme *b*. Asp, Gly, Met, Ala and the porfirine ring of heme *b* were also recognized in van der Waals contact with the quinone molecule [47]. Quite often, an acidic residue is present in the

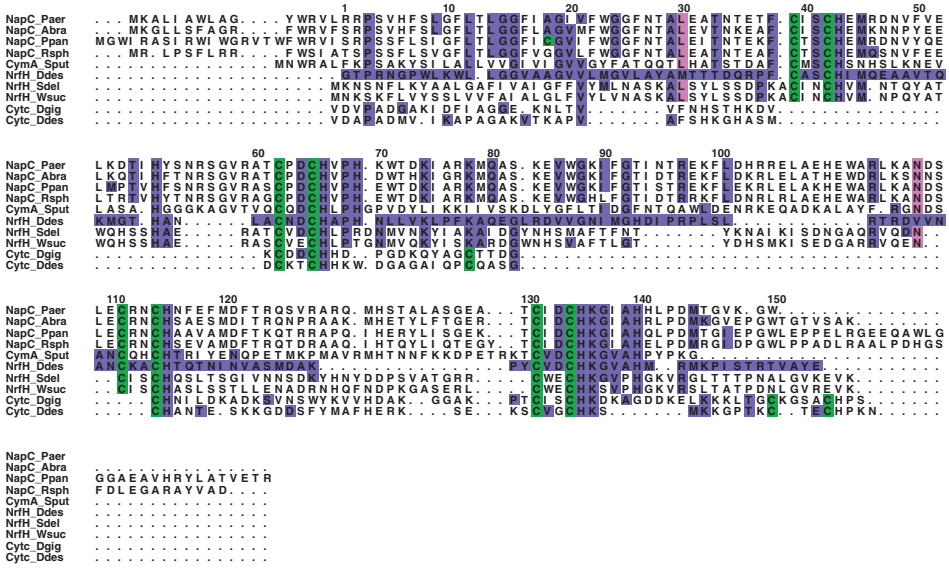

Fig. 4. Sequence alignment of NrfH from *D. desulfuricans* ATCC 27774 with members of the NapC/NirT family and cytochrome c_3 from *Desulfovibrio* species. Cysteines are coloured in green, NrfH_Ddes conserved amino-acid sequence and residues are marked in purple, residues conserved in members of the NapC/NirT family but not in NrfH_Ddes are indicated in pink. NapC_Paer, NapC from *Pseudomonas aeruginosa* (TREMBL Q9I4G5); NapC_Abra, NapC from *Azospirillum brasilense* (TREMBL Q8VU45); NapC_Ppan, NapC from *Paracoccus pantotropha* (SWISS-PROT Q56352); NapC_Rsph, NapC from *Rhodobacter sphaeroides* (TREMBL O88116); CymA_Sput, CymA from *Shewanella putrefaciens* (TREMBL P95832); NrfH_Ddes: NrfH from *D. desulfuricans* ATCC 27774, NrfH_Sdel: NrfH from *S. deleyianum* (TREMBL Q8VM54), NrfH_Wsuc: NrfH from *W. succinogenes* (TREMBL Q9S1E6), Cytc_Dgig: cyt c_3 from *D. gigas* (SWISS-PROT P00133), Cytc_Ddes: cyt c_3 from *D. desulfuricans* ATCC 27774 (SWISS-PROT P00134). The figure was prepared with the programs ALSCRIPT [55] and CLUSTALW [56].

quinone-binding pocket, probably acting as a proton shuttle [45,46]. Recent crystallographic studies on quinone:fumarate reductase from *W. succinogenes* [48] and *E. coli* K-12 [49] highlighted the role of Glu in the quinone/quinol site constitution. As the selected NrfH segment provides several amino acids fulfilling the above description, we propose that the putative quinone-binding pocket of NrfH is near its soluble domain, probably in close contact with heme 1, which is partially embedded in the membrane, hence facilitating the electron flow.

Spectroscopy

As isolated in SDS, NrfA and NrfH display a typical cytochrome *c*-type UV-Vis spectra (not shown).

The X-band EPR spectra (10 K) of both subunits in the presence of SDS are quite similar to each other (Fig. 5). Two main signals were observed: a high-spin Fe(III) ($S = 5/2$) at $g = 6.1$ and a typical low-spin ($S = 1/2$) ferric heme at $g = 2.96$, 2.26 and 1.50. However, the high-spin contribution to the total NrfH spectrum is minor (Fig. 5B), suggesting that the four heme irons in this subunit are in a low-spin state.

The high-spin species well detected in NrfA (Fig. 5A) should correspond to a magnetically isolated form of the heme previously assigned to the substrate-binding site [23]. In addition, a derivative-type signal with zero crossing at $g = 4.28$ is assigned to nonspecific bound iron.

These EPR spectral features are comparable to the ones observed for the *D. desulfuricans* ATCC 27774 ccNiR complex in the presence of SDS [19]. In fact, all the coupling signals observed in the EPR of the native enzyme (see Introduction) disappeared following the incubation in this detergent. This phenomenon was attributed to the denaturation action of SDS [19].

The EPR of the native complex exhibits a derivative-type signal with zero-crossing at $g = 4.8$ [23] that is absent in the spectra of ccNiR preparations from the soluble fraction of other organisms such as *E. coli* K-12 [16], *W. succinogenes* and *S. deleyianum* [13], exclusively constituted by the periplasmic NrfA subunit. This resonance should be originated by internal magnetic coupling from NrfH hemes or, if in close proximity to the NrfA, could arise from spin coupling between hemes from both subunits.

Reassessment of the Mössbauer data

The *D. desulfuricans* ATCC 27774 ccNiR Mössbauer spectra obtained in the presence of a strong magnetic field were originally interpreted as a superposition of six spectral components of equal intensity (16.6%) and distinct hyperfine parameters (at the time the enzyme was considered as a monomer containing six *c*-type hemes) [23]. Following our present analysis, the enzyme is a complex of two different subunits – the pentahemic NrfA and the tetrahemic NrfH, implying the existence of nine different hemes. Thus, a re-evaluation of the Mössbauer data (native state and samples poised at different reduction potentials), recorded at 4.2 K and 8 T, was undertaken, considering that ccNiR samples comprise

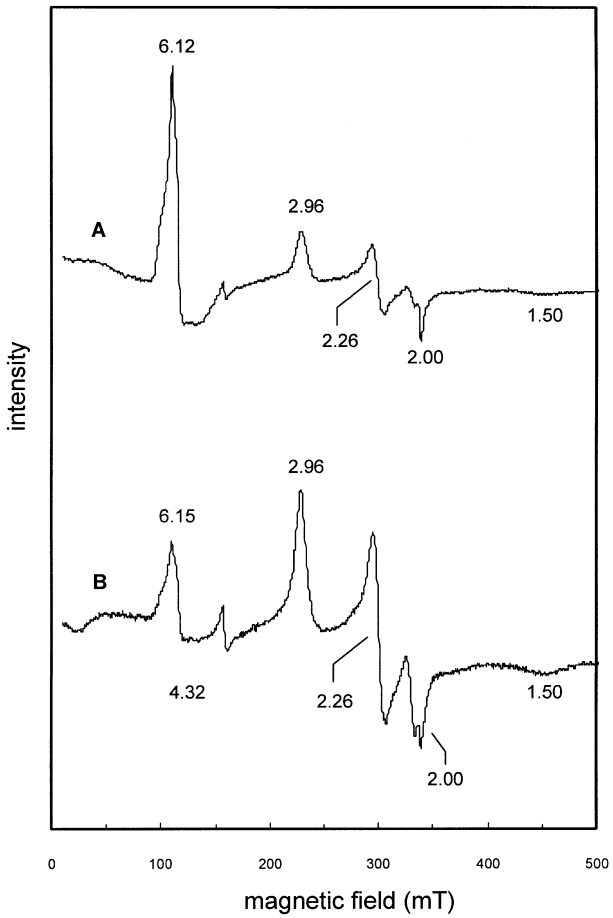

Fig. 5. X-Band EPR spectra of *D. desulfuricans* ATCC 27774 ccNiR subunits, as isolated by gel filtration chromatography in the presence of 1% SDS (in 0.1 M Tris/HCl pH 7.6). (A) NrfA; (B) NrfH. Temperature, 10 K; microwave frequency, 9.5 GHz; microwave power, 2 mW; modulation amplitude, 1 mT.

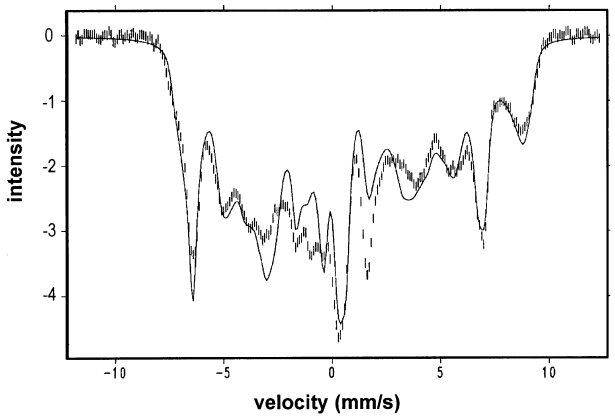

Fig. 6. Mössbauer spectra of *D. desulfuricans* ATCC 27774 ccNiR native complex (pH 7.6). The solid lines correspond to theoretical simulations using parameters reported in [24], and assuming a subunit content of two NrfA to one NrfH. Temperature, 4.2 K; applied field parallel to the γ-beam, 8 T.

two NrfA to one NrfH subunits. According to this stoichiometry, each NrfA heme corresponds to 14% of the total iron absorption, and each NrfH heme corresponds to 7%. From previous EPR studies [23], two sets of low-spin ferric *g*-values (g_{max} at 2.96 and 3.20) and a high-spin heme were observed, here assigned to the NrfA subunit and therefore, contributing with 14% each.

The Mössbauer spectrum (Fig. 6) reveals low-spin components with extremely large magnetic splittings, characteristic of low-spin species with g_{max} higher than 3.3. In order to fit these outer regions of the experimental spectra, we used three different components, two from the NrfA subunit and one from NrfH, according to the following considerations. The original Mössbauer studies on NrfHA complex identified two low-spin hemes with g_{max} values at 3.60 and 3.50. The work of Walker *et al.* on low-spin ferric heme model compounds with axial imidazole ligands correlated the g_{max} values larger than 3.3 with perpendicularly aligned axial imidazole planes [50]. As the NrfA crystal structure shows two *bis*-His ligated hemes with orthogonal imidazole geometry [17], we assigned the $g_{max} = 3.60$ and 3.50 signals to the NrfA subunit, each contributing with 14%. At this stage, all the five hemes from NrfA were taken into account in the new simulation (70% of total iron absorption). Though, the next components were attributed to the small NrfH subunit. The contribution of 28%, from the NrfA subunit, to the large g_{max} low spin-hemes ($g_{max} > 3.3$) intensity was considerably less than the experimental value (35%). Hence, it was necessary to add a third component with $g_{max} = 3.55$ and an intensity of 7%. According to the redox titration followed by Mössbauer spectroscopy, this low-spin ferric heme should have a positive reduction potential: it is titrated after the complete reduction of the $g_{max} = 3.50$ heme ($E'_m = +150$ mV vs. SHE), and before reaching a potential of 0 mV (note that the $g_{max} = 3.60$ low-spin heme has a very low reduction potential [24]). Finally, as already reported in [23], to obtain agreement between the experimental data and the theoretical simulations, it is necessary to include a low-spin ferric heme component with g_{max} between 2.96 and 3.20. For this reason, a value of g_{max} 3.00 was chosen for the remaining three hemes from the small NrfH subunit, hence contributing with $3 \times 7\%$ to the total intensity. All the parameters used in this simulation were the same as indicated previously [24].

In the first publication [23], the authors noticed that a better agreement could be obtained if the contribution of the high-spin heme was reduced from 16.6% to 14%. To explain it, they proposed that the high-spin heme content was less than one or, the recoilless fractions for the high-spin and the low-spin hemes were different [23]. Now, we have found an absolutely different justification, related to the new biochemical characterization.

In conclusion, we have shown that the proposed Mössbauer spectra simulation, based on the actual biochemical characterization of *D. desulfuricans* ATCC 27774 ccNiR complex (NfrHA), plus several structural considerations on NrfA, fit as well as the former simulation as they do to the experimental data. The large subunit NrfA, contains the high-spin heme, and four low-spin *c*-hemes with $g_{max} = 3.6$, 3.50, 3.2 and 2.96, while the NrfH subunit

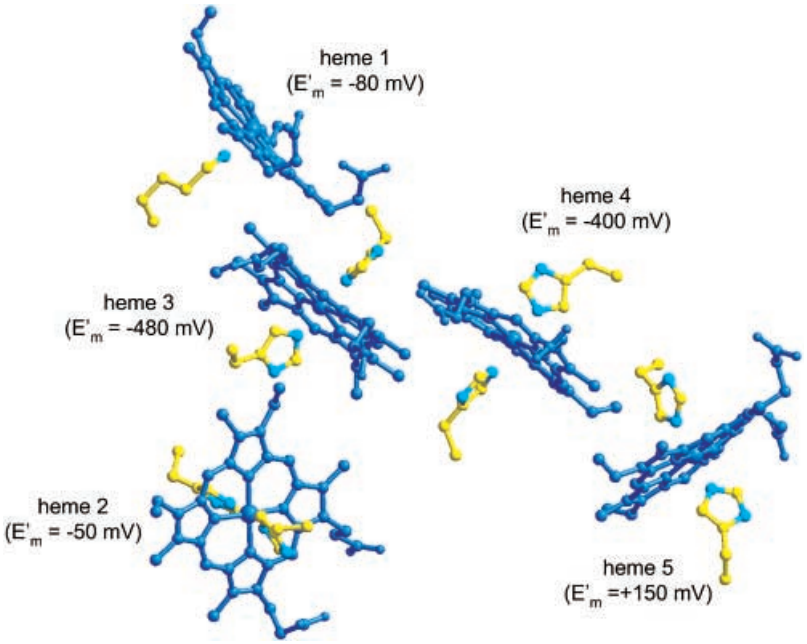

Fig. 7. Relative spatial arrangement of *D. desulfuricans* ATCC 27774 NrfA hemes groups. The assignment of midpoint reduction potentials to individual hemes was based on spectroscopic considerations, combined with the following structural data (taken from [17]). Axial histidines angles (°): heme 2, 23.3; heme 3, 54.6; heme 4, 74.8; heme 5, 78.8. Fe-Fe distances (Å): hemes 1–3, 9.59; hemes 2–3, 12.52; hemes 1–4, 16.74; hemes 4–5, 11.16; hemes 3–4, 9.67; hemes 5–5 (dimer), 11.11. Solvent accessibility (Å^2): heme 1, 34.0; heme 2, 96.0; heme 3, 2.5; heme 4, 3.0; heme 5, 70.0. The figure was prepared with the programs MOLSCRIPT AND RASTER3D [57,58].

Table 2. Heme assignment of *D. desulfuricans* ATCC 27774 ccNiR subunits. The NrfA hemes were numbered according to the aminoacid sequence. The NrfH hemes designation was aleatory; hemes H_2 to H_4 are indistinguishable from the spectroscopy point of view.

Subunit	Heme	g_{max}	E'_m (mV)[a]
NrfA	1	6.12	−80
	2	2.96	−50
	3	3.20	*c.*−480
	4	3.60	*c.*−400
	5	3.50	+150
NrfH	H_1	3.55	> 0
	H_2, H_3, H_4	3.00	*c.*−300

[a] vs. SHE.

encloses four heme groups in a low-spin configuration, one with $g_{max} = 3.55$ and a positive midpoint reduction potential (> 0 mV), and three with $g_{max} = 3.00$, with a midpoint reduction potential of approximately −300 mV (Table 2).

Spectroscopy and structure correlations

The determination of the 3D structure of *D. desulfuricans* ATCC 27774 NrfA [17] enabled to ascertain the spatial characterization of the five hemes, namely their proximity and the axial histidine plane angles (Fig. 7). A correlation between individual hemes obtained spectroscopic (EPR and Mössbauer) signals, with known reduction potentials, and was then undertaken.

Heme 1 (according to *D. desulfuricans* ATCC 27774 NrfA amino-acid numbering) has the sixth axial position vacant. Thus, is the site of substrate interaction (high-spin heme, −80 mV). The EPR results revealed that this heme is pairwise coupled with a $g_{max} = 3.20$ low-spin heme [23]. Regarding the distance and the relative orientation to heme 1 (Fig. 7), the stronger candidate to couple is heme 3 (approximately −480 mV). Heme 2 (−50 mV) is the one with g_{max} of 2.96 that is EPR detectable and is magnetically isolated. Structurally, it is distant from the remaining hemes and the dihedral angles of the axially coordinated His support this assignment (Fig. 7, interplanar angles in legend). The Mössbauer data reveals the presence of two low-spin ferric hemes with large g_{max} (3.50 and 3.60). The hemes that satisfy such requirements are hemes 4 and 5 (Fig. 7, legend). One of these hemes is magnetically isolated (g_{max} 3.50) [24]. As hemes 1, 3 and 4 are almost coplanar and heme 5 is slightly apart, this latter heme is, probably, the magnetically isolated one. As seen by UV-Vis and Mössbauer spectroscopy, this heme is reduced at a positive reduction potential (+150 mV) that is unusual for a heme with *bis*-His axial ligation. Heme 4 should have g_{max} at 3.60 and reduction potential of approximately −400 mV.

Due to high reduction potential and heme solvent exposure, we also propose heme 5 as the site of electron entrance from its redox partner NrfH (Fig. 7, legend). The solvent exposure calculations did not consider the presence of the NrfH subunit; the presence of this integral membrane subunit will decrease the solvent accessibility of hemes 2 and 5, which are located near the putative surface contact [17]. The redox potential of *c*-type cytochromes can be tuned by approximately 500 mV through variations in the heme exposure to solvent [51,52]. The encapsulation of the heme group in a hydrophobic environment causes a positive shift in the reduction potential, up to approximately 240 mV in cytochrome *c* [52]. This may explain the atypical positive reduction potential of heme 5, if in close proximity with the hydrophobic transmembrane NrfH subunit. However, these suggestions are purely speculative and heme 2 should not be excluded as a candidate for the electron entrance, as postulated [15,16].

In the NrfH subunit, it was not possible to perform the structural assignment of the heme spectroscopic and reduction potentials information, as there are no structures available for NrfH like proteins or any member of the

NapC/NirT family. Nevertheless, crystals of *W. succinogenes* NrfHA complex have been recently reported [53]. Table 2 describes the relationship between the heme core description and the spectroscopic and redox properties of each identified heme from the NrfHA complex.

Conclusions

D. desulfuricans ATCC 27774 ccNiR is isolated as a mixture of high molecular mass hetero-oligomeric complexes, constituted by a large pentahemic NrfA subunit, and a transmembrane tetrahemic NrfH subunit. The *in vitro* subunit stoichiometry is two NrfA to one NrfH. However, micellar chromatography experiments suggested that the smallest physiological heterooligomeric unit is most probably a $\alpha_2\beta_2$ complex.

NrfA is the catalytic subunit and is active as a functional dimer. NrfH should be involved in the transfer of electrons from the cytoplasmic membrane to NrfA, located at the periplasm side. ccNiRs are, in general, periplasmic membrane-associated proteins, but in some species (see Introduction), a soluble form exclusively composed by the large NrfA subunit could also be isolated. We found no experimental evidences of a *D. desulfuricans* ATCC 27774 ccNiR soluble form. One might infer from these results that the enzyme topology should be somewhat different in each proteobacteria subdivision. Actually, in the γ-proteobacteria, both catalytic NrfA subunit and its electron donor NrfB are soluble proteins [22]. No stable NrfAB complex was isolated from *E. coli* K-12 cells [16]. In the ε-group members, such as *W. succinogenes* and *S. deleyianum*, the large NrfA subunit shows a peripheral membrane topology, solely bound to the membrane by the NrfH transmembrane subunit. Therefore, can easily detach to the periplasm or become partly solubilized during breaking up of the cells. In other species, as the δ-proteobacterium *D. desulfuricans* ATCC 27774, the NrfA is firmly bound to the membrane, by a putative covalently thioether-bonded lipid of a N-terminal cysteine residue, reinforced by a strong interaction with the periplasmic oriented membrane anchored NrfH subunit, as experimentally demonstrated by the difficulties in separating them. The strong interaction between the two subunits persists even in the presence of harsh denaturating reagents. Only SDS was able to completely dissociate the complex into its monomers and, even so, it did not completely eliminate the enzymatic activity as seen by SDS/PAGE gel stained for nitrite reductase activity. It should be noticed that attempts to separate the components of ccNiR complex from *D. vulgaris* Hildenborough (also a member of the δ-subdivision) were unsuccessful or led to the degradation of the isolated species [10]; as a consequence, the stoichiometry of the complex was not established. The formation of stable NrfHA complexes in the ε-proteobacteria and especially in the δ-subdivision members should be advantageous to the bacteria, as it would facilitate the efficient electron transfer from the proposed electron donor, quinone pool [47], to the catalytic site.

The analysis of NrfH sequence reveals that this protein has two putative domains: a soluble one comprising three Class III *c*-type hemes (hemes 2–4), and a hydrophobic domain, inserted in the cytoplasmic membrane featuring a fourth heme (heme 1) probably involved in the quinol oxidation.

The present work, in combination with previous spectroscopic studies [23,24] and with *D. desulfuricans* ATCC 27774 NrfA heme core description reported in [17], allowed for the first time, the complete association between magnetic signals and midpoint reduction potentials to each of the five different hemes. It was definitively established that NrfA hemes exhibit a broad range of reduction potentials, spanning from −480 to +150 mV (pH 7.6). Heme 5 has an unusual positive reduction potential for a *bis*-His axial coordination, also seen by redox titrations followed by UV-Vis spectroscopy in NrfHA complex from *D. vulgaris* Hildenborough (+ 150 mV) [10] and in NrfA from *E. coli* K-12 (+ 45 mV) [54]. This is the first complete description of midpoint reduction potentials of heme prosthetic groups from an NrfA protein. A previous attempt to correlate the spectroscopic signals and midpoint reduction potentials to individual hemes of *E. coli* K-12 NrfA structure was recently carried out by Bamford *et al.* [16]. However, the insufficient spectral EPR resolution of electrochemically poised samples, and the lack of Mössbauer information (no data on uncoupled hemes), hampered the complete assignment. In fact, heme 2 (g_{max} 2.91) was the only one with an unequivocal reduction potential attribution (−37 mV), which is quite close to the corresponding value in NrfA (−50 mV). The magnetic coupling signal assigned to hemes 1 and 3 titrates at −107 mV. A g_{max} 3.17 (−323 mV) signal was ascribed to hemes 4/5 [16]; by comparison with our proposition, this signal should belong to heme 4. No attribution was made to the positive reduction potential formerly seen.

The novel Mössbauer analysis led to the description of previously unobserved spectroscopic features, namely, a heme of $g_{max} = 3.55$, with a positive midpoint reduction potential (> 0 mV), and three heme groups at $g_{max} = 3.00$ with a midpoint reduction potential of approximately −300 mV, all assigned to the formerly uncharacterized NrfH subunit.

Acknowledgements

We thank to Prof B. Devreese from Laboratorium voor eiwitbiochemie en eiwitengineerin, Universiteit Gent, for the MALDI spectra. We also thank to Prof B. H. Huynh from Department of Physics, Emory University, for his collaboration on the original Mössbauer studies.

This work was financially supported by FSE and FCT (Fundação para a Ciência e Tecnologia), through the PhD grants PRAXIS XXI/BD/11349/97 (GA), PRAXIS XXI/BD/16009/98 (SM) and PRAXIS XXI/BD/15752/98 (CAC), and by the COST working group.

References

1. Zumft, W.G. (1997) Cell biology and molecular basis of denitrification. *Microbiol. Mol. Biol. Rev.* **61**, 533–616.
2. Bercks, B.C., Ferguson, S.J., Moir, J.W.B. & Richardson, D.J. (1995) Enzymes and associated electron transport systems that catalyse the respiratory reduction of nitrogen oxides and oxyanions. *Biochim. Biophys. Acta* **1232**, 97–173.
3. Liu, M.C. & Peck, H.D. (1981) The isolation of a hexaheme cytochrome from *Desulfovibrio desulfuricans* and its identification as a new type of nitrite reductase. *J. Biol. Chem.* **256**, 13159–13161.

4. Kajie, D. & Anraku, Y. (1986) Purification of a hexaheme cytochrome c_{552} from *Escherichia coli* K12 and its properties as a nitrite reductase. *Eur. J. Biochem.* **154**, 457–463.
5. Rehr, B. & Klemme, J.H. (1986) Metabolic role and properties of nitrite reductase of nitrate-ammonifying marine *Vibrio* species. *FEMS Microbiol. Lett.* **35**, 325–328.
6. Liu, M.C., Bakel, B.W., Liu, M.Y. & Dao, T.N. (1988) Purification of *Vibrio fischeri* nitrite reductase and its characterization as a hexaheme c-type cytochrome. *Arch. Biochem. Biophys.* **262**, 259–295.
7. Liu, M.C., Liu, M.Y., Payne, W.J., Peck, H.D. & LeGall, J. (1983) *Wolinella succinogenes* nitrite reductase: purification and properties. *FEMS Microbiol. Lett.* **19**, 201–206.
8. Schumacher, W. & Kroneck, P.M.H. (1991) Dissimilatory hexaheme *c* nitrite reductase of '*Spirillum*' strain 5175: purification and properties. *Arch. Microbiol.* **156**, 70–74.
9. Murillo, M.F., Gugliuzza, T., Senko, J., Basu, P. & Stolz, J.F. (1999) Heme *c*-containing complex that exhibits nitrate and nitrite reductase activity from the dissimilatory iron reducing bacterium, *Geobacter metallireducens*. *Arch. Microbiol.* **172**, 313–320.
10. Pereira, I.C., LeGall, J., Xavier, A.V.M. & Teixeira, M. (2000) Characterization of a heme *c* nitrite reductase from a non-ammonifying microorganism, *Desulfovibrio vulgaris* Hildenborough. *Biochim. Biophys. Acta* **1481**, 119–130.
11. Barton, L.L., LeGall, J., Odom, J.M. & Peck, H.D. (1983) Energy coupling to nitrite respiration in the sulfate-reducing bacterium *Desulfovibrio gigas*. *J. Bacteriol.* **153**, 867–871.
12. Darwin, A., Hussain, H., Griffiths, L., Grove, J., Sambong, Y., Busby, S. & Cole, J. (1993) Regulation and sequence of the structural gene for cytochrome c_{552} from *Escherichia coli*: not a hexahaem but a 50 kDa tetrahaem nitrite reductase. *Mol. Microbiol.* **9**, 1255–1265.
13. Schumacher, W., Hole, U. & Kroneck, P.M.H. (1994) Ammonia-forming cytochrome *c* nitrite reductase from *Sulfurospirillum deleyianum* is a tetraheme protein: new aspects of the molecular composition and spectroscopic properties. *Biochem. Biophys. Res. Commun.* **205** (1), 911–916.
14. Einsle, O., Messerschmidt, A., Stach, P., Bourenkov, G.P., Bartunik, H.D., Huber, R. & Kroneck, P.M.H. (1999) Structure of cytochrome *c* nitrite reductase. *Nature* **400**, 476–480.
15. Einsle, O., Stach, P., Messerschmidt, O.A., Simon, J., Kröger, A., Huber, R. & Kroneck, P.M.H. (2000) Cytochrome *c* nitrite reductase from *Wolinella succinogenes*. *J. Biol. Chem.* **275**, 39608–39616.
16. Bamford, V.A., Angove, H.C., Seward, H.E., Thomson, A.J., Cole, J.A., Butt, J.N., Hemmings, A.M. & Richardson, D.J. (2002) Structure and spectroscopy of the periplasmic cytochrome *c* nitrite reductase from *Escherichia coli*. *Biochemistry* **41**, 2921–2931.
17. Cunha, C.A., Macieira, S., Dias, J.M., Almeida, M.G., Gonçalves, L.M.L., Costa, C., Lampreia, J., Huber, R., Moura, J.J.G., Moura, I. & Romão, M. (2003) Cytochrome *c* nitrite reductase from *Desulfovibrio desulfuricans* ATCC 27774. The relevance of the two calcium sites in the structure of the catalytic subunit (NrfA). *J. Biol. Chem.* **278**, 17455–17465.
18. Pereira, I.C., Abreu, I.A., Xavier, A.V.M., LeGall, J. & Teixeira, M. (1996) Nitrite reductase from *Desulfovibrio desulfuricans* (ATCC 27774) – a heterooligomer heme protein with sulfite reductase activity. *Biochem. Biophys. Res. Commun.* **224**, 611–618.
19. Moura, I., Bursakov, S., Costa, C. & Moura, J.J.G. (1997) Nitrate and nitrite utilization in sulfate-reducing bacteria. *Anaerobe* **3**, 279–290.
20. Almeida, G., Lampreia, J., Moura, J.J.G. & Moura, I. (1999) New biochemical studies on nitrite reductase from *Desulfovibrio desulfuricans* ATCC 27774. *J. Inorg. Biochem.* **74**, 63.
21. Simon, J., Gross, R., Einsle, O., Kroneck, P.M., Kroger, A. & Klimmek, O. (2000) A NapC/NirT-type cytochrome *C* (NrfH) is the mediator between the quinone pool and the cytochrome *C* nitrite reductase of *Wolinella succinogenes*. *Mol. Microbiol.* **35**, 686–696.
22. Hussain, H., Grove, J., Griffiths, L., Bersby, S. & Cole, J. (1994) A seven-gene operon essential for formate-dependent nitrite reduction to ammonia by enteric bacteria. *Mol. Microbiol.* **12**, 153–163.
23. Costa, C., Moura, J.J.G., Moura, I., Liu, M.-Y., Peck, H.D., LeGall, J., Wang, Y. & Huynh, B.H. (1990) Hexaheme nitrite reductase from *Desulfovibrio desulfuricans*. Mössbauer and EPR characterization of the heme groups. *J. Biol. Chem.* **254**, 14382–14387.
24. Costa, C., Moura, J.J.G., Moura, I., Wang, Y. & Huynh, B.H. (1996) Redox properties of cytochrome *c* nitrite reductase from *Desulfovibrio desulfuricans* ATCC 27774. *J. Biol. Chem.* **271**, 23191–23196.
25. Liu, M.C., Costa, C. & Moura, I. (1994) Hexaheme nitrite reductase from *Desulfovibrio desulfuricans* (ATCC 27774). *Methods Enzymol.* **243**, 303–319.
26. Dias, J.M., Cunha, C.A., Almeida, G., Costa, C., Lampreia, J., Moura, J.J.G., Moura, I. & Romão, M.J. (2000) Crystallization and preliminary X-ray analysis of a membrane-bound nitrite reductase from *Desulfovibrio desulfuricans* ATCC 27774. *Acta Crystallogr.* **D56**, 215–217.
27. Laemmli, U.K. (1970) Cleavage of structural proteins during the assembly of the head of bacteriophage T4. *Nature* **227**, 680–685.
28. Blum, H., Beier, H. & Gross, H.J. (1987) Improved silver staining of plant proteins, RNA and DNA in polyacrylamide gels. *Electrophoresis* **8**, 93–99.
29. Goodhew, C.F., Brown, K.R. & Pettigrew, G.W. (1986) Haem staining in gels, a useful toll in the study of bacterial *c*-type cytochromes. *Biochim. Biophys. Acta* **852**, 288–294.
30. Manchenko, G.P. (1994) *Handbook of Detection of Enzymes on Electrophoretic Gels* pp. 86. CRC Press, Boca Raton, FL, USA.
31. Fuhrop, J.H. & Smith, K.M. (1975) In *Laboratory Methods – Porphyrins and Metalloporphyrins* (Smith K.M., eds.), pp. 804–807. Elsevier, Amesterdam, the Netherlands.
32. Nicholas, D.J.D. & Nason, A. (1957) Determination of nitrate and nitrite. *Methods Enzymol.* **3**, 981–984.
33. Sonnhammer, E.L.L., Heijne, G.V. & Krogh, A. (1998) A hidden Markov model for predicting transmembrane helices in protein sequences. In *Proceedings of the of 6th International Conference on on Intelligent Systems for Molecular Biology*, pp. 175–182. AAAI Press, CA, USA.
34. Simon, J., Pisa, R., Stein, T., Eichler, R., Klimmek, O. & Gross, R. (2001) The tetraheme cytochrome *c* NrfH is required to anchor the cytochrome *c* nitrite reductase (NrfA) in the membrane of *Wolinella succinogenes*. *Eur. J. Biochem.* **268**, 5776–5782.
35. Hayashi, S. & Wu, H.C. (1990) Lipoproteins in bacteria. *J. Bioenerg. Biomembr.* **22**, 451–471.
36. Roldán, M.D., Sears, H.J., Cheesman, M.R., Ferguson, S.J., Thomson, A.J., Berks, B.C. & Richardson, D.J. (1998) Spectroscopic characterization of a novel multiheme *c*-type cytochrome widely implicated in bacterial electron transport. *J. Biol. Chem.* **273**, 28785–28790.
37. Liu, M.C., Costa, C., Coutinho, I.B., Moura, J.J.G., Moura, I., Xavier, A.V. & LeGall, J. (1988) Cytochrome components of nitrate- and sulfate-respiring *Desulfovibrio desulfuricans* ATCC 27774. *J. Bacteriol.* **170**, 5545–5551.
38. Moura, I., Costa, C., Liu, M.Y., Moura, J.J.G. & LeGall, J. (1991) Structural and functional approach toward a classification of the complex cytochrome *c* system found in sulfate-reducing bacteria. *Biochim. Biophys. Acta* **1058**, 61–66.

39. Morais, J., Palma, P.N., Frazão, C., Caldeira, J., LeGall, J., Moura, I., Moura, J.J. & Carrondo, M.A. (1995) Structure of the tetraheme cytochrome from *Desulfovibrio desulfuricans* ATCC 27774: X-ray diffraction and electron paramagnetic resonance studies. *Biochemistry* **34**, 12830–12841.
40. Norager, S., Legrand, P., Pieulle, L., Hatchikian, C. & Roth, M. (1999) Crystal structure of the oxidised and reduced acidic cytochrome c_3 from *Desulfovibrio africanus*. *J. Mol. Biol.* **290**, 881–902.
41. Czjzek, M., Guerlesquin, F., Bruschi, M. & Haser, R. (1996) Crystal structure of a dimeric octaheme cytochrome c_3 (M_r 26 000) from *Desulfovibrio desulfuricans* Norway. *Structure* **15**, 395–404.
42. Czjzek, M., Arnoux, P., Haser, R. & Shepard, W. (2001) Structure of cytochrome c_7 from *Desulfuromonas acetoxidans* at 1.9 Å resolution. *Acta Crystallogr.* **D57**, 670–678.
43. Assfalg, M., Banci, L., Bertini, I., Bruschi, M. & Turano, P. (1998) 800 MHZ. ^{1}H NMR solution structure refinement of oxidized cytochrome c_7 from *Desulfuromonas acetoxidans*. *Eur. J. Biochem.* **256**, 261–270.
44. Fisher, N. & Rich, P. (2000) A motif for quinone binding sites in respiratory and photosynthetic systems. *J. Mol. Biol.* **296**, 1153–1162.
45. Hägerhäll, C. (1997) Succinate: quinone oxidoreductases. Variations on a conserved theme. *Biochim. Biophys. Acta* **1320**, 107–141.
46. Westenberg, D.J., Gunsalus, R.P., Ackrell, B.A.C., Sices, H. & Cecchini, G. (1993) *Escherichia coli* fumarate reductase frdC and frdD mutants. Identification of amino acid residues involved in catalytic activity with quinones. *J. Biol. Chem.* **268**, 815–822.
47. Jormakka, M., Törnroth, S., Byrne, B. & Iwata, S. (2002) Molecular basis of proton motive force generation: structure of formate dehydrogenase-N. *Science* **295**, 1863–1868.
48. Lancaster, C.R.D., Groβ, R., Haas, A., Ritter, M., Mäntele, W., Simon, J. & Kröger, A. (2000) Essential role of Glu-C66 for menaquinol oxidation indicates transmembrane electrochemical potential generation by *Wolinella succinogenes* fumarate reductase. *Proc. Natl Acad. Sci. USA* **97**, 13051–13056.
49. Iverson, T.M., Luna-Chavez, C., Croal, L.R., Cecchini, G. & Rees, D.C. (2002) Crystallographic studies of the *Escherichia coli* quinol-fumarate reductase with inhibitors bound to the quinol-binding site. *J. Biol. Chem.* **277**, 16124–16130.
50. Walker, F.A., Huynh, B.H., Scheidt, R. & Osvath, S.R. (1986) Models of the cytochromes *b*6. The effect of axial ligand plane orientation on the EPR and Mössbauer spectra of low-spin ferrihemes. *J. Am. Chem. Soc.* **108**, 5288–5297.
51. Kennedy, M.L. & Gibney, B.R. (2001) Metalloprotein and redox protein design. *Curr. Op. Struct. Biol.* **11**, 485–490.
52. Tezcan, F.A., Winkler, J.R. & Gray, H.B. (1998) Effects of ligation and folding on reduction potentials of heme proteins. *J. Am. Chem. Soc.* **120**, 13883–13388.
53. Einsle, O., Stach, P., Messerschmidt, O.A., Klimmek, O., Simon, J., Kröger, A. & Kroneck, P.M.H. (2002) Crystallization and preliminary X-ray analysis of the membrane-bound cytochrome *c* nitrite reductase complex (NrfHA) from *Wolinella succinogenes*. *Acta Crystallogr.* **D58**, 341–342.
54. Eaves, D.J., Grove, J., Standenmamm, W., James, P., Poole, R.K., White, S.A., Griffiths, I. & Cole, J.A. (1998) Involvement of products of the nrfEFG genes in the covalent attachment of haem *c* to a novel cysteine-lysine motif in the cytochrome c_{552} nitrite reductase from *Escherichia coli*. *Mol. Microbiol.* **28**, 205–216.
55. Barton, G.J. (1993) ALSCRIPT: a tool to format multiple sequence alignments. *Protein Eng.* **6**, 37–40.
56. Thompson, J.D., Higgins, D.G. & Gibson, J. (1994) The CLUSTAL_X windows interface: flexible strategies for multiple sequence alignment aided by quality analysis tools. *Nucleic Acids Res.* **22**, 4673–4680.
57. Kraulis, P.J. (1991) MOLSCRIPT: a program to produce both detailed and schematic plot of protein structures. *J. Appl. Cryst.* **24**, 946–950.
58. Merrit, E.A. & Bacon, D.J. (1997) In *Macromolecular Crystallography, Part B*. (Carter, C.W. & Sweet, R.M., eds), pp. 505–524. Academic Press, New York, USA.